Atmospheric Research 285 (2023) 106640

Contents lists available at ScienceDirect

Atmospheric Research

journal homepage: www.elsevier.com/locate/atmosres

How much of precipitation over the Euroregion Galicia – Northern Portugal is due to tropical-origin cyclones?: A Lagrangian approach

Albenis Pérez-Alarcón [a,b,*], José C. Fernández-Alvarez [a,b], Rogert Sorí [a], Margarida L.R. Liberato [c,d], Ricardo M. Trigo [c,e], Raquel Nieto [a], Luis Gimeno [a]

[a] Centro de Investigación Mariña, Universidade de Vigo, Environmental Physics Laboratory (EPhysLab), Campus As Lagoas s/n, Ourense 32004, Spain
[b] Departamento de Meteorología, Instituto Superior de Tecnologías y Ciencias Aplicadas, Universidad de La Habana, 10400 La Habana, Cuba
[c] Instituto Dom Luiz, Faculdade de Ciências da Universidade de Lisboa, 1749-016 Campo Grande, Portugal
[d] Escola de Ciências e Tecnologia, Universidade de Trás-os-Montes e Alto Douro, Vila Real, Portugal
[e] Departamento de Meteorologia, Universidade Federal do Rio de Janeiro, Rio de Janeiro, 21941-919, Brazil

ARTICLE INFO

Keywords:
Tropical cyclones
Precipitation
Rainfall contribution
Moisture sources
Lagrangian approach
Euroregion Galicia-Northern Portugal

ABSTRACT

This study analyses the contribution of the tropical-origin cyclones (TCs) to monthly rainfall amounts in the Euroregion Galicia–Northern Portugal (EG-NP) from 1980 to 2018, while simultaneously determines the moisture sources that generate this TCs-related precipitation over the EG-NP region. We quantified the amount of rainfall contributed by TCs using the high resolution Multi–Source Weighted–Ensemble Precipitation dataset, and the identification of the sources of moisture was performed by applying a Lagrangian diagnostic method. The EG-NP region was impacted by 30 TCs during the study period, distributed from August to November, with September and October showing the highest frequency, with 10 and 13 TCs respectively. Mostly, TCs influenced the study region after undergoing an extratropical transition, however, a few well know events, such as Ophelia (October 2017) and Leslie (October 2018) still impacted with hurricane category 1 on the Saffir-Simpson wind scale. On average, the TCs-related precipitation accounted for ~4.2% of mean rainfall from August to November, although September with ~7.1% exhibited the largest contribution. Likewise, the highest TCs-related rainfall was found towards the western and northern region of EG-NP. Furthermore, during the passage dates, TCs obtained most of the precipitating moisture (~75%) from the subtropical North Atlantic Ocean. On the other, the traditional climatological moisture sources for the EG-NP came from the Atlantic coast of Morocco and the Iberian Peninsula during August and October, from the western Mediterranean Sea in September, and a weak pattern from the Cantabrian Sea in November. These findings could be useful for future studies on understanding the possible impacts caused by TCs in this region in a warmer climate.

1. Introduction

Tropical-origin cyclones, known as tropical cyclones (TCs), are weather systems that every year not only provoke natural disasters in tropical regions but also in mid-latitudes (Evans et al., 2017; Zhao et al., 2018; Bieli et al., 2019; Keller et al., 2019). The increasing population density in coastal areas, the significant modification of coastal zones and the development of infrastructures in these areas increase the vulnerability to TCs impacts.

The formation and development of TCs are controlled by atmospheric and ocean large-scale circulations (e.g. weak vertical wind shear, sea surface temperature, ocean surface feedback, ocean heat content and mid-level humidity), microscale cloud microphysical processes and vortex-scale convective circulations (Wang and Wu, 2004; Hendricks et al., 2010; Montgomery and Smith, 2017). Additionally, it is well known that climate variability modes influence TC activity by controlling large-scale atmospheric and ocean conditions. As expected, the El Niño – Southern Oscillation (ENSO) coupled pattern plays a major role in terms of TC variability. For example, during the warm phase (El Niño) the genesis of TCs is reduced in the North Atlantic Ocean (NATL), but it is enhanced during the cold phase or La Niña (Landsea, 2000; Bell et al., 2014; Patricola et al., 2014; Boudreault et al., 2017; Klotzbach et al., 2017). Meanwhile, several authors have confirmed that the positive phase of the North Atlantic Oscillation (NAO) suppresses the frequency

* Corresponding author at: Edificio Campus da Auga. Universidade de Vigo, Campus Sur. Rúa Canella da Costa da Vela 12, 32004 Ourense, Spain.
E-mail address: albenis.perez.alarcon@uvigo.es (A. Pérez-Alarcón).

https://doi.org/10.1016/j.atmosres.2023.106640
Received 7 November 2022; Received in revised form 3 January 2023; Accepted 29 January 2023
Available online 1 February 2023

of TC genesis in NATL (Elsner et al., 2000; McCloskey et al., 2013; Zhang et al., 2022). In addition, TCs trajectories are modulated by the large-scale steering flow linked to the strength and position of the North Atlantic Subtropical High (NASH) pressure system. Colbert and Soden (2012) noted that during El Niño and positive NAO, the NASH weakens and shifts eastward, which results in anomalous cyclonic flow in the eastern mid-Atlantic, increasing the frequency of recurving TCs and thus the probability that a TC may impact western Europe.

1.1. Motivation and state of the art

Despite their destructive capacity, TCs play a key role in the hydrological cycle over the tropical and mid-latitudes regions (Jiang and Zipser, 2010; Kam et al., 2013; Khouakhi et al., 2017; Yang et al., 2018), contributing significantly to total rainfall amounts. For example, TCs-related precipitations represent ~10–30% of total rainfall over East Asia (Guo et al., 2017), ~20–40% over northern Australia (Dare et al., 2012), ~11% over Cuba (Fernández-Alvarez et al., 2020), and ~ 8–12% along the southeastern United States coast (Prat and Nelson, 2013). Khouakhi et al. (2017) found that TCs account for 35% - 50% of the mean annual rainfall in northwestern Australia, southeastern China, the northern Philippines, and Baja California (Mexico). Xu et al. (2017) showed that the NATL basin and Eastern Pacific TCs contributed ~14% and ~ 19% of total moisture flux onto North America, respectively. Through a global study, Jiang and Zipser (2010) found that the TCs' contribution to total rainfall accounted for ~3–4%, ~5%, ~7%, ~7–8%, ~8–9%, and ~ 11% in the South Pacific, Northern Indian Ocean, East Central Pacific, Southern Indian Ocean, NATL, and Western North Pacific basins, respectively. This study also revealed that TCs contribute approximately 5% of the mean annual rainfall in the Iberian Peninsula (IP), especially in the Euroregion Galicia – Northern Portugal (EG-NP). Most recently, Baker et al. (2021) studied the variability of NATL tropical and post-tropical cyclones over mid-latitude regions, revealing that ~25% and ~10% of TCs made landfall across northeastern North America and Europe, respectively, and Tan et al. (2022) noted that rapid intensification process in TCs tend to increase TC-related extreme rainfall over land.

During poleward propagation, TCs lose their tropical characteristics and often undergo extratropical transition caused by colder ocean water and changes in the mid-latitude environment (Hart and Evans, 2001; Evans et al., 2017). Nevertheless, some TCs can influence the weather in western Europe with strong winds and intense rainfall (Hickey, 2011). The last decade has been characterized by a rise of TCs in the NATL sector, with an increase in TCs that describe a trajectory that brought them closer to the Azores archipelago or even the northwestern IP (Lima et al., 2021). Some TCs recurving to the northeastern in the central NATL are steered by the westerly winds to the vicinity of the IP coast and Great Britain. For example, TC Ophelia, in October 2017, rose further northern than any other category 2 Hurricane (maximum sustained wind speed on surface ranging from 154 to 177 km/h) on the Saffir-Simpson wind scale and eventually struck Ireland with strong winds of approximately 190 km/h, killing at least three people (Altman et al., 2018; Stewart, 2018). Another important example of TCs that moved circa the western IP coast was TC Lorenzo on October 2019, which is considered the most intense TC observed in the eastern NATL basin (Zelinsky, 2019; Lima et al., 2021). Recently, remnants TC Danielle in September 2022 caused heavy precipitation on the western coast of Portugal (see Floods in Portugal at https://floodlist.com/europe/portugal-floods-manteigas-september-2022).

Studies related to TCs in mid-latitudes have been commonly focused on the analysis of the structural changes during extratropical transitions (Studholme et al., 2015; Evans et al., 2017; Bieli et al., 2019; Laurila et al., 2019). Several authors have also pointed out that the rising of the sea surface temperature (SST) due to global warming modifies the incidence of TCs (Emanuel et al., 2008; Emanuel and Sobel, 2013; Manganello et al., 2014; Balaguru et al., 2016; Knutson et al., 2019) and, thus, it is expected an increase in the risk of damage caused by these events in mid-latitudes (Haarsma et al., 2013). Indeed, previous research findings (Zhao and Held, 2012; Murakami et al., 2012; Daloz and Camargo, 2018; Sharmila and Walsh, 2018; Studholme and Gulev, 2018) highlighted that global warming causes a poleward and eastward extension of the TCs genesis areas in the NATL basin, explained by changes in convection or the poleward extension of the Hadley Cell circulation (Sharmila and Walsh, 2018; Studholme and Gulev, 2018). These projections imply that future TCs could increasingly influence extreme storm conditions in mid-latitudes, and thus, an increased likelihood of western Europe being hit by strong storms is expected (Haarsma et al., 2013; Dekker et al., 2018). In addition, Baatsen et al. (2015) showed from model simulations that future TCs reattain a lower warm core when impacting Europe, which implies the hazards of both tropical and extratropical systems.

Based on projections for TC activity in a warmer climate, the geographical position of the IP makes it more vulnerable to the impact of these storms (Baatsen et al., 2015). In this context, it is expected to observe an increment in the contribution of TCs to the precipitation totals in the IP, which could be more noticeable in the EG-NP. Therefore, this study seeks to examine the contribution of TCs to monthly rainfall amounts in the EG-NP. This goal will be addressed using a gridded precipitation dataset and identifying the moisture contributions for precipitation associated with TCs over the EG-NP. For the latter purpose, the extensively used Lagrangian approach (see Gimeno et al., 2012, 2020, and references therein) was applied using the FLEXible PARTicle (FLEXPART) dispersion model (Stohl et al., 2005), due to its skillful for tracking atmospheric particles in space and time (Winschall et al., 2014). This approach has been previously used to study the moisture source for meteorological systems such as low-level jets (Algarra et al., 2019; Zhang et al., 2019; Braz et al., 2021), atmospheric rivers (Liberato et al., 2012; Algarra et al., 2020), and a range of cyclone types, including extratropical (Liberato et al., 2013; Papritz et al., 2021; Coll-Hidalgo et al., 2022a), Mediterranean (Flaounas et al., 2019; Coll-Hidalgo et al., 2022b) and tropical (Pérez-Alarcón et al., 2022a, 2022b, 2022c, 2022d) cyclones.

The results should contribute to a better understanding of the expected changes in the hydrological cycle in the EG-NP region linked to TCs activity under a warmer climate. The paper is organized as follows. Section 2 provides a detailed description of the data, methods and the Lagrangian moisture source identification method, while the results and discussion are presented in Section 3. Finally, the paper ends with the conclusions and plans for future works in Section 4.

1.2. Study area

The EG-NP, with a surface of 50,853 km^2, is a cross-border region located at northwestern IP (Pardellas and Padín, 2017) characterized by a complex terrain (Ćurić et al., 2003). Politically it englobes the autonomous northwest Spanish community of Galicia (composed by four Provinces: Pontevedra, Ourense, Coruña and Lugo) and the northern region of Portugal (composed by the sub-regions of Minho-Lima, Cávado, Ave, Grande Porto, Tâmega, Entre Douro e Vouga, Douro, and Trás-os-Montes e Alto Douro regions). The EG-NP extends from 40.5°N to 44°N in latitude and 6°W to 9.5°W in longitude (Fig. 1).

The EG-NP is bounded by the North Atlantic Ocean and the Cantabrian Sea, which implies a high oceanic influence on the climate of coastal and adjacent areas (Lorenzo et al., 2010a, 2010b), with mild summers and rainy winters; however, the interior of the region is characterized by a continental climate, with dry summers and cold winters (Gómez-Gesteira et al., 2011). This region is commonly impacted by extratropical cyclones (Trigo, 2006) and cut-off-low systems (Nieto et al., 2007), and the intensity of winter precipitation is influenced by the orography near the coastline. Furthermore, the advection of cold and moist air masses from the North Atlantic Ocean frequently characterize its autumn season (Valero et al., 2009). Previous

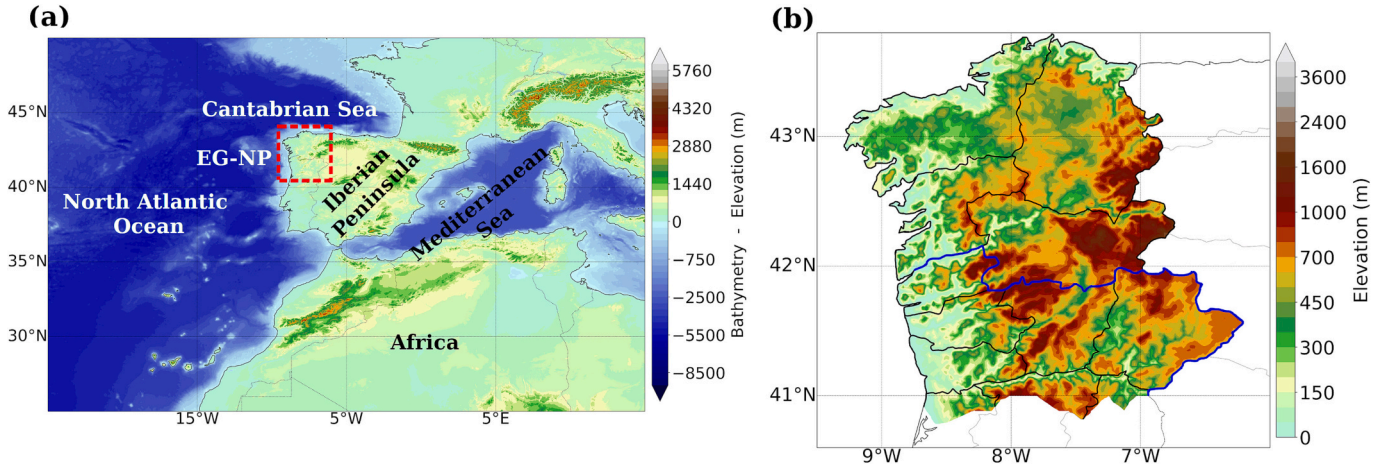

Fig. 1. **(a)** Geographic location of Euroregion Galicia – Northern Portugal (EG-NP, red box) in the Iberian Peninsula. **(b)** Zoom of EG-NP region. The boundaries of Galicia provinces and northern Portugal subregions are delimited with solid black line, while the blue solid line represents the boundary between Spain and Portugal in the EG-NP region. The topography data was obtained from https://www.ngdc.noaa.gov/mgg/global/global.html (For interpretation of the references to colour in this figure legend, the reader is referred to the web version of this article.)

studies have shown that the variability of precipitation and temperature is influenced by climatic variability modes such as NAO and also by ENSO (Lorenzo and Taboada, 2005; de Castro et al., 2006; Trigo et al., 2008; Lorenzo et al., 2010a; Ramos et al., 2010). In addition, Sorí et al. (2020) noted that hydrological droughts are mainly controlled by dry and wet conditions at shorter and mid-to-long-term temporal scales, with a marked influence during the rainy months (December–April).

2. Materials and methods

2.1. Data

The North Atlantic hurricane database (HURDAT2; Landsea and Franklin, 2013) was used to extract the TCs position every 6 h. This database contains TC data since 1851. However, according to several authors (Vecchi and Knutson, 2008, 2011; Kossin et al., 2013; Schreck et al., 2014; Delgado et al., 2018; Bhatia et al., 2019), the quality and robustness of these historical records is considerably higher after the beginning of the meteorological satellite era in the later 1970s. The TC size was obtained from the TCSize database developed by Pérez-Alarcón et al. (2021, 2022d) using the radial wind profile developed by Willoughby et al. (2006).

To determine the rainfall amounts that the TCs produced in comparison with the monthly climatology over the EG-NP and to compute the Standardized Precipitation Index (SPI), the daily precipitation totals from the Multi–Source Weighted–Ensemble Precipitation (MSWEP) database in version 2 (Beck et al., 2019) was used. The MSWEP has a spatial resolution of 0.1° x 0.1° in latitude and longitude, and 3 h of temporal resolution. This dataset combines data from many sources such as gauge stations, satellite and reanalysis data, and it is freely available from 1979.

To identify the moisture sources for TCs-related precipitation over the EG-NP, the global outputs from the FLEXPART model (Stohl et al., 2005) were used. FLEXPART simulations were performed by the Environmental Physics Laboratory (EPhysLab) of the Universidade de Vigo, Spain. These FLEXPART model outputs have been used extensively for similar purposes by this research group in the last decade (see Gimeno et al., 2012, 2020 and references therein). The model was fed by the 6-hourly ERA-Interim reanalysis (Dee et al., 2011) from the European Centre for Medium Range Weather Forecasting (ECMWF) at 1° x 1° of horizontal resolution and on 61 vertical levels. For the model simulations approximately 2 million particles were homogeneously globally distributed and dispersed following the 3D wind fields. The model runs were performed in a spacing grid of 1° in latitude and longitude and the same vertical levels of the input data. In addition, as global models are unable to resolve individual convective cells, the model used the convection parameterization proposed by Emanuel and Živković-Rothman (1999) to account for subgrid-scale convective transport. Likewise, to account for turbulence in the planetary boundary layer (PBL), FLEXPART solved Langevin equations for Gaussian turbulence (Stohl and Thomson, 1999). The PBL height was determined using a combination of the Richardson number and the lifting parcel technique (Vogelezang and Holtslag, 1996). The FLEXPART outputs (including parcel position and specific humidity) are available every 6 h from January 1980 to July 2019.

Based on the time span of the different datasets, the study period was set from 1980 to 2018. Furthermore, to gain a physical insight of the moisture transport mechanisms that transported the atmospheric humidity from the moisture sources towards the TCs location and the EG-NP, the vertical integrated moisture flux (VIMF) was computed every 6 h from the vertically integrated northward and eastward moisture fluxes from ERA-I reanalysis data. Additionally, as the recurving TCs frequency is modulated by ENSO and NAO (e.g. Colbert and Soden, 2012; McCloskey et al., 2013; Sainsbury et al., 2022), the Oceanic Niño Index (ONI) based on Niño 3.4 region (5°S–5°N, 170°–120°W) and the NAO index (Jones et al., 1997) were used to investigate if these modes modulate the frequency of TCs in the EG-NP region.

2.2. Methodology

2.2.1. Identification of TCs that reached the Euroregion Galicia – Northern Portugal and assessment of its impacts

In this study, a TC was conserved to have influenced the EG-NP region if, along its trajectory, at least once, the region was inner the TC outer radius. Previous studies used ~500–600 km as a distance fixed threshold for the TC outer radius definition (Englehart and Douglas, 2001; Jiang and Zipser, 2010; Dominguez and Magaña, 2018; Zhang et al., 2018; Fernández-Alvarez et al., 2020), although all of them were performed for tropical regions. According to previous works, TCs increase in size during their poleward propagation as a response to environmental changes that favor baroclinic growth at the expenses of the more compact and symmetric barotropic behavior of typical TCs (Hart and Evans, 2001; Kimball and Mulekar, 2004; Pérez-Alarcón et al., 2021). Therefore, the outer radius of TCs from the TCSize database was used as distance threshold to determine if a TC impacted the EG-NP region.

To evaluate the influence of ENSO and NAO on TC passage over or near the EG-NP region, TC events were grouped during the positive and negative phase of both climate modes. A TC season was classified as El Niño, La Niña or neutral phase using the ONI. That is, if there are five consecutive months of the year in which the 3-month running mean ONI is greater (lower) than 0.5 °C (−0.5 °C), that year was classified as an El Niño (La Niña) season. Otherwise, it was categorized as a neutral TC season. This approach has been previously applied in several works (e.g. Colbert and Soden, 2012; Bhardwaj et al., 2019). In addition, TCs that influenced the EG-NP were separated into positive and negative phases of NAO (without a neutral class), according to the NAO phase at the TC genesis time, in agreement with Colbert and Soden (2012).

2.2.2. *Identification of moisture sources for TCs-related precipitation*

To identify the origin of TCs-related precipitation along the TCs trajectories during the considered days to the EG-NP region, the moisture source diagnostic method developed by Sodemann et al. (2008) was used. This moisture tracking method has been recently implemented in the TRansport Of water Vapor (TROVA) tool (Fernández-Alvarez et al., 2022). Here we do not separate the moisture uptake obtained from the atmospheric boundary layer and that from the free atmosphere. The method is based on the Lagrangian approach to the humidity budget (Stohl and James, 2004, 2005), in which the atmospheric moisture content can be modified by moisture gains or losses due to evaporation or precipitation, respectively. In contrast to Stohl and James (2004, 2005) formulation, TROVA proportionally discounts precipitation en route to all earlier moisture uptakes (MUs) by evaluating individually the particles backward trajectories from the end to the start point. The air parcel trajectories from the previously described FLEXPART model global outputs were used.

As our focus is the final precipitation within the TC outer radius, the precipitant particles over the target region were backtracked in time for up to 10 days (the mean water vapor residence time in the atmosphere (Numaguti, 1999; van Der Ent and Tuinenburg, 2017; Gimeno et al., 2021)). The precipitant particles are defined as those in which the specific humidity decreases by >0.1 g/kg before arriving at the target region (Läderach and Sodemann, 2016). As commented previously, the target region is the area enclosed by the outer radius of each TC position according to the TCSize database during the TCs passages dates.

Furthermore, the kernel density estimation (KDE; Rosenblatt, 1956; Parzen, 1962) was used to gain an overview of the trajectories of precipitant particles linked to TCs-related precipitation over the EG-NP region. The KDE is a non-parametric technique for estimation of probability density function (PDF; Węglarczyk, 2018). The widely applied Gaussian kernel (Wahiduzzaman and Yeasmin, 2020) was chosen for our purposes as it is computationally efficient and assumes a uniform relationship between the variables under consideration (Eckert-Gallup and Martin, 2016).

3. Results and discussion

3.1. *TCs that impacted the Euroregion Galicia – Northern Portugal*

The trajectories of the TCs that reached EG-NP during the study period (1980 to 2018) are shown in Fig. 2a. During this period, 598 TCs were formed over the NATL basin, but only 30 TCs (~5%) influenced the EG-NP region according to our criterion. Previously, Baker et al. (2021) using reanalysis datasets found that approximately 10% of NATL TCs from 1979 to 2018 impacted the European coastline. The annual frequency of TCs in the North Atlantic basin that impacted the EG-NP region (Fig. 2b) reveals that the highest frequency occurred in 1998 and 2018, with 4 and 3 TCs, respectively. Generically, those TCs influencing the EG-NP region can be classified as “recurving ocean TCs”, according to the track classification of Colbert and Soden (2012); interestingly, only one TC formed in the Caribbean Sea (Michael (AL142018)) impacted the EG-NP. Fig. 2a also reveals that seven of the TCs identified

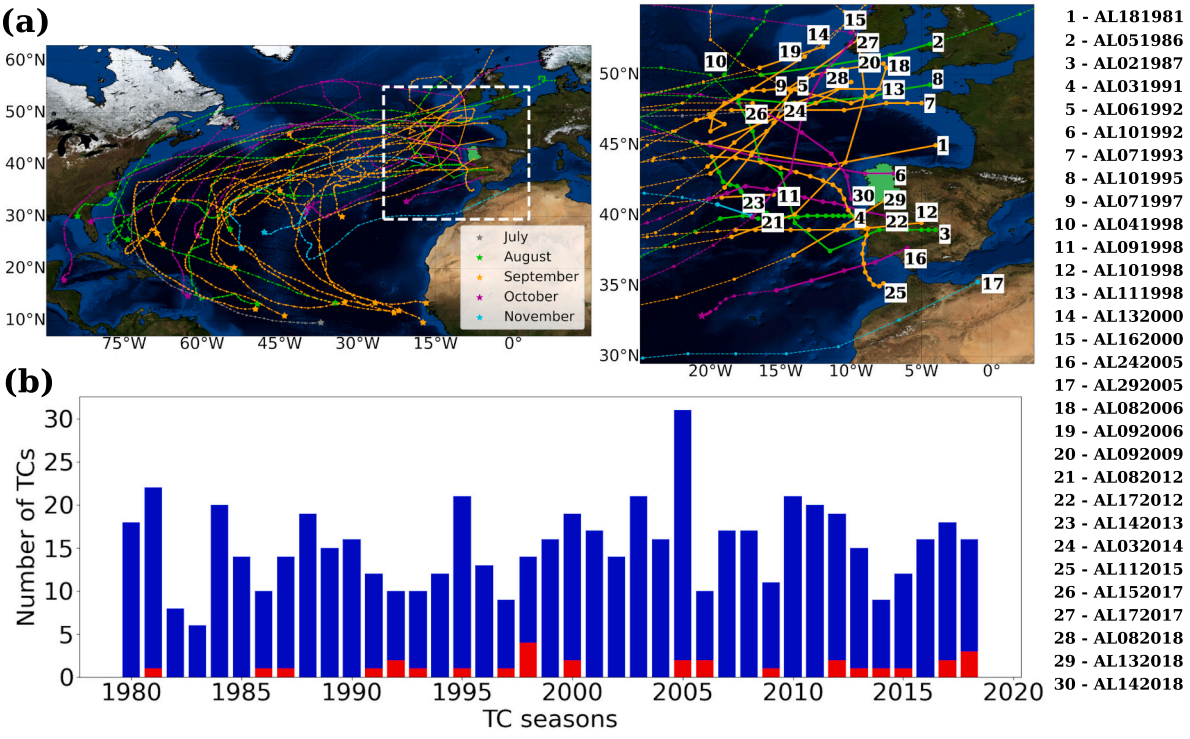

Fig. 2. **(a)** Trajectory of the 30 TCs that impacted the Euroregion Galicia – Northern Portugal (EG-NP, highlighted in light-green). The dashed coloured lines (for each genesis month) represent the full TC trajectory and the stars represent the genesis point. The trajectories in solid lines represent the part of the track where the outer radio of each individual TC impacts the EG-NP region. **(b)** Annual frequency of TCs in the whole North Atlantic basin (in blue) and the subgroup that impacted the EG-NP region (in red). (For interpretation of the references to colour in this figure legend, the reader is referred to the web version of this article.)

(~23%) made landfall in the IP and only one of them in the EG-NP (Frances (AL101992)).

Additionally, the monthly frequency exhibits 5 TCs in August, 10 in September, 13 in October and only 2 in November. It is worth noting that TCs generally impacted the EG-NP region at the end of their lifetime (see Fig. 2a), thus, the monthly genesis frequency of those TCs notably differ from the monthly frequency of influence. Indeed, TCs that impacted the EG-NP region were commonly formed in September (15 TCs), followed by August and October (6 TC each month), November (2 TCs) and July (only 1), as indicated in Fig. 2a.

This work also explored the linkages between ENSO and NAO and the frequency of TCs that impacted the EG-NP region, counting the number of TCs during both warm and cold phases. We found that 23.3% (20.0%) of TCs impacts occurred under El Niño (La Niña) conditions, and no large differences were found during both phases of NAO, 43.3% during positive NAO and 56.7% in the negative phase. These results suggest that ENSO and NAO do not modulate TCs influence on the EG-NP region.

The main characteristics of each single TC that impacted the EG-NP region and their stage of evolution when they impacted the region are displayed in Table 1. Most of the TCs impacted the EG-NP during their extratropical stage (EX), with the exception of Ophelia (AL172017) and Leslie (AL132018) that impacted first as hurricanes category 1 (maximum sustained wind speed on surface ranging from 119 to 153 km/h) on the Saffir-Simpson scale (HU1), and later during their extratropical stage, Vince (AL242005) as tropical storm, and Gordon (AL082012) as a low pressure system. The occurrence of a few hurricanes that have made landfall in recent years is in line with results by Lima et al. (2021) that have confirmed the increasing occurrence of stronger TCs and hurricanes in the region around Azores and Iberia. Regarding their intensities, they ranged from 55 to 120 km/h during the extratropical stage or tropical storm category, being higher, as it is expected, during hurricane category, from 120 to 148 km/h.

3.2. TC rainfall contribution to Euroregion Galicia – Northern Portugal

The spatial patterns of monthly rainfall over the EG-NP, from August to November 1980–2018 are presented in Fig. 3. The climatological average rainfall for each month (Fig. 3a) shows that August is the driest month in the region, with mean rainfall amounts ranging from 40 to 50 mm in northern EG-NP, and <30 mm in the southern part. Besides, the mean monthly rainfall ranges from 75 to 100 mm in September in the central region, while in October and November the monthly rainfall varies from 125 to 225 mm. In these last two months, the highest accumulated precipitations are located in the central-western part of the EG-NP in October and spread across the western coast in November. Overall, the highest monthly rainfall is located towards the western EG-NP. These results agree with previous studies (Lorenzo and Taboada, 2005; de Castro et al., 2006), who found that the precipitation in EG-NP is characterized by a maximum in winter, from November to February, and a minimum in summer, from June to August.

The monthly average rainfall only including those years in which occurred a TC reaching the EG-NP is depicted in Fig. 3b. All four maps reveal that the average precipitation is clearly higher than the corresponding long-term average rainfall in the whole study period. In October and November, the mean rainfall associated to the TCs reached values higher than 275 mm in most of the EG-NP region. Meanwhile, over the central-northern EG-NP ranged from 100 to 175 mm in August and November.

Additionally, the monthly average TC-related precipitation, and the percentage of the TCs contribution to the monthly average rainfall concerning the years in which a TC passage occurred are shown in Fig. 3c and Fig. 3d, respectively. In August, the average TCs-related precipitation ranges from 3 mm to 5 mm in the most sectors of the EG-NP (Fig. 3c), but reached up to 10–12.5 mm in western Galicia, representing ~5–6% of total monthly mean precipitation (Fig. 3d). September and October both showed a similar spatial pattern, with the

Table 1
Tropical-origin cyclones (TCs) characteristics that impacted the Euroregion Galicia – Northern Portugal (EG-NP) from HURDAT2 database in the period 1980–2018. The maximum wind (km/h) refers to the wind peak registered by the TC during the passage dates, and the stage indicates the TC phases, EX: Extratropical stage (TC undergo extratropical transition), HU_1: Category 1 hurricane (maximum sustained wind speed on surface ranging from 119 to 153 km/h) on the Saffir–Simpson wind scale, TS: Tropical Storm, LO: low system that is neither a TC, a subtropical cyclone, nor an extratropical cyclone (of any intensity).

Year	TC Code	TC Name	Impact start s	Impacts ends	Maximum wind (km/h)	Stage
1981	AL181981	Irene	2 October	3 October	83.30	EX
1986	AL051986	Charley	25 August	26 August	92.50	EX
1987	AL021987	Arlene	25 August	28 August	83.30	EX
1991	AL031991	Bob	23 August	29 August	55.30	EX
1992	AL061992	Charley	28 September	29 September	83.30	EX
	AL101992	Frances	29 October	30 October	74.00	EX
1993	AL071993	Floyd	11 September	13 September	115.2	EX
1995	AL101995	Iris	6 September	7 September	120.1	EX
1997	AL071997	Erika	18 September	19 September	111.1	EX
1998	AL041998	Danielle	6 September	6 September	111.2	EX
	AL091998	Ivan	27 September	27 September	83.30	EX
	AL101998	Jeanne	2 October	4 October	74.10	EX
	AL111998	Karl	28 September	29 September	64.80	EX
2000	AL132000	Isaac	3 October	3 October	110.1	EX
	AL162000	Leslie	10 October	10 October	111.0	EX
2005	AL242005	Vince	10 October	11 October	83.30	TS
	AL292005	Delta	29 November	29 November	55.50	EX
2006	AL082006	Gordon	21 September	24 September	120.0	EX
	AL092006	Helene	26 September	27 September	83.00	EX
2009	AL092009	Grace	5 October	6 October	101.7	TS, EX
2012	AL082012	Gordon	21 August	21 August	83.30	LO
	AL172012	Rafael	24 October	26 October	74.00	EX
2013	AL142013	Melissa	23 November	23 November	64.80	EX
2014	AL032014	Bertha	9 August	9 August	64.80	EX
2015	AL112015	Joaquin	9 October	15 October	83.30	EX
2017	AL152017	Maria	2 October	2 October	55.50	EX
	AL172017	Ophelia	15 October	16 October	148.0	HU_1, EX
2018	AL082018	Helene	17 September	17 September	92.50	EX
	AL132018	Leslie	13 October	14 October	120.0	HU_1, EX
	AL142018	Michael	10 October	15 October	101.7	EX

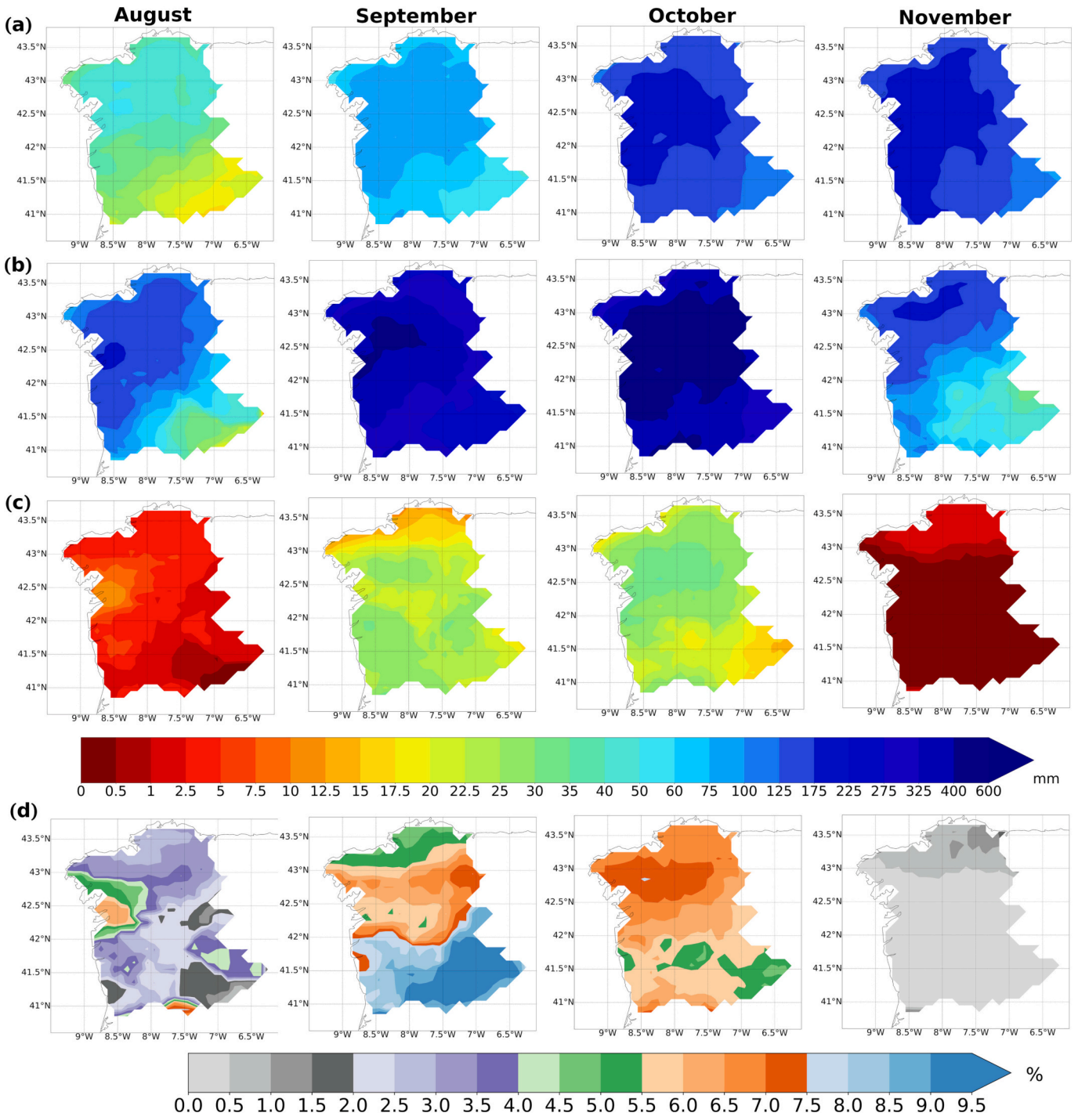

Fig. 3. **(a)** Climatological average monthly rainfall in the Euroregion Galicia - Northern Portugal in the period 1980–2018 from August to November, **(b)** Like (a), but only including the years at which a TC passage occurred, **(c)** Average monthly TC-related precipitation during the TC passage days, (**d)** Percentage of contribution of TCs to the monthly average rainfall, computed as the fraction between (c) and (b). Precipitation data from the MSWEP database for the period 1980–2018.

largest TC-related precipitation occurring in October, when the northern EG-NP receives between 25 and 35 mm. Meanwhile, in September the southeastern EG-NP accumulated between 20 and 30 mm (Fig. 3c). In terms of percentage (Fig. 3d), the highest contribution to the monthly rainfall occurred in September, ranging from 5% to 9% from north to south, being higher than 9.5% in the southeastern EG-NP, while in October the contribution varied in the opposite latitudinal direction, with lower percentages being observed in the south than in the north, ranging from 5% to 7.5%, respectively. In general, these findings revealed that the western and northern coastal areas of the EG-NP received the largest TCs rainfall contribution (in agreement with previous studies (e.g. Khouakhi et al., 2017)), which can be explained by the TCs trajectories (see Fig. 2a) during the passage dates. In addition, as TCs rarely impacts the study region in November (only two cases), the TC-related precipitation represented less than ~1.0% of the mean rainfall and confined to northern EG-NP.

A summary of these results can be appreciated in Fig. 4, that shows the monthly average rainfall for August, September, October and November (blue bars) and monthly mean TCs-related precipitation (red bars) from the monthly rainfall only including years at which a TC

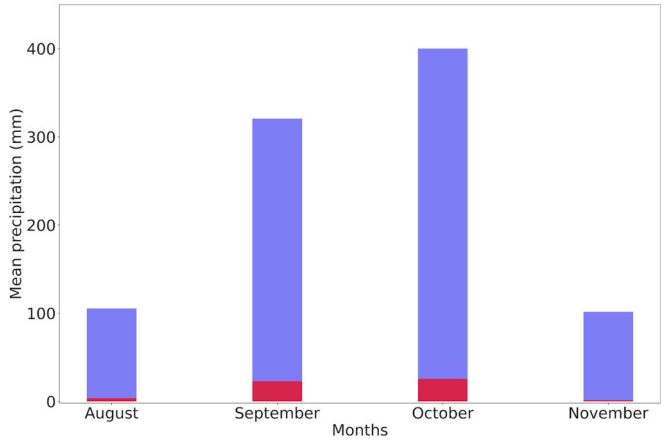

Fig. 4. Average monthly rainfall over the Euroregion Galicia - Northern Portugal including the years at which a TC passage occurred (blue bars) and monthly mean TCs-related precipitation (red bars). These overall metrics were calculated by averaging the rainfall on land grid points from the MSWEP precipitation database for the period 1980–2018. (For interpretation of the references to colour in this figure legend, the reader is referred to the web version of this article.)

passage occurred in the EG-NP region. The increment in total mean precipitation from August (105.3 mm) to October (399.9 mm) is quite notably. Similarity, the TC-related precipitation increases from August (3.5 mm) to October (25.2 mm), but notably decreases in November (0.36 mm). The proportion of TC-induced rainfall accounted for ~3.3% in August, ~7.1% in September, ~6.2% in October, and less than ~0.5% in November. On average, the TCs-related precipitation amounts represented approximately 4.2% of the mean rainfall in these four months. This finding agrees with the results of Khouakhi et al. (2017) in a global scale study.

However, the relatively low average contribution of a few TCs to monthly precipitation affecting the EG-NP region, as shown in Fig. 4, can be slightly misleading. In fact, the few months that were indeed affected by a TC may have registered an important contribution to the monthly rainfall. Fig. 5a shows the contribution to the monthly rainfall during the passage of each TC listed in Table 1. The TC Gordon (AL082006) achieved the largest contribution in an individual month, September 2006, accounting for ~51.7% (~60.1 mm) of mean monthly rainfall. Conversely to the monthly average previously discussed, the Gordon rainfall was higher on the southeastern EG-NP ranging from 75 to 105 mm (Fig. 5b), which represents approximately 65–80% of the total precipitation of September 2006 in this area. The second and third TCs that most contributed to the monthly rainfall in the EG-NP region were Frances (AL101992, October 1992) and Leslie (AL132018, October 2018), respectively, which, according to historical records of the HURDAT2 database (see Fig. 2a), the first made landfall in the northwestern EG-NP and both dissipated over the study region. The average Frances related precipitation (~45 mm) represented ~35% of the mean total rainfall in October 1992, while the mean rainfall amount registered during Leslie influence (~31.4 mm) accounted for ~31% of mean rainfall total in October 2018. Fig. 5c and Fig. 5d also reveal the spatial distribution of total precipitations during October 1992 and 2018, and the contribution of Frances and Leslie, respectively. The higher rainfall totals related to Frances (Fig. 5c) were found across the northeastern EG-NP, representing about 40–50% of the monthly rainfall. For Leslie, although the largest amounts of precipitation were located northeastward, the highest contribution (~35–45%) to monthly rainfall was detected in the central mountainous region. Finally, it is worth highlighting the case of TC Bob (AL031991), which contributed ~30% to the accumulated precipitations during August 1991 (Fig. 5a) with the highest related precipitation being recorded in the northern half of EG-NP, with a maximum on the west coast of Galicia, providing between ~40–60% (Fig. 5b). However, Bob was responsible for most of the total precipitation in parts of the southeastern corner of the EG-NP (>90%). The contributions of the remaining TCs that impacted the EG-NP region were <25%, and it is easily verified that the lowest contributions correspond to TCs that passed furthest from the study region (see the trajectories in Fig. 2a).

We would like to stress that the apparent low contribution of TCs towards the precipitation in the EG-NP results to a large extent from the type of comparison performed in both Figs. 3 and 5. In those figures, the contribution of monthly precipitation (i.e. during months impacted by TCs) towards the corresponding total monthly precipitation was evaluated. The relatively small number of TCs influencing the precipitation in this region implies that their contribution is restricted to just a few days during a small number of years, and therefore, their overall contribution to the total monthly accumulated precipitation is necessarily small (<8%) as summarized in Fig. 4. However, if the same assessment is performed, comparing the average EG-NP precipitation produced by TCs with the climatological value for the same days, then its contribution raises substantially to 82% (August), 272% (September) and 170% (October). Nevertheless, we acknowledge that these apparently very high values can also be misleading, as they result from the fact summer months are climatologically dry in the EG-NP region. Thus, average long-term precipitation of 3 mm can be easily doubled (6 mm) during months affected by TCs.

3.3. The origin of TCs-related precipitations

To identify the origin of TCs-related precipitation during the dates of TCs passage (Fig. 6 left panel) in the EG-NP region, the Lagrangian moisture source diagnostic tool TROVA to the precipitant atmospheric particle trajectories from the global outputs of the FLEXPART model was applied. The right panel of Fig. 6 shows the monthly composite climatological moisture uptake and VIMF patterns for the precipitation within the TC outer radius.

No large differences are observed in the moisture sources for TCs-related precipitation over the whole area influenced by the TC size from August to November (Fig. 6, right panel). The highest moisture contribution (~80%) came from the region spanning between 33°–55° N and 0°–40° W in the mid-latitudes and subtropical North Atlantic Ocean, close to the Atlantic IP coast. Nevertheless, the moisture uptake pattern is more intense and widespread during September than during October and August, probably due to the concentration of the TC trajectories during the period of influence. Likewise, the core of moisture sources is slightly shifted to the south in October respect to August and September. In addition, TCs in September gained moisture from the remote source located over the eastern coast of the United States, meanwhile, the North Atlantic Ocean above 20° N of latitude and around the nuclei of maximum moisture uptake weakly contributed. Interestingly, the western part of the IP appears also as a moisture source, being more significant in August (~3.5–4 mm/day) and September (~2.5–3 mm/day) than in October (~1.5–2 mm/day). The VIMF pattern during the period of TCs influenced the EG-NP region from August to October (Fig. 6a-c).

As rarely TCs influenced the EG-NP region during November and the trajectories described by the two TCs were different (Fig. 6d), the moisture uptake pattern is notably different from that observed from August to October. Despite this, again the central NATL acted as the main moisture source, supplying more than ~65% of the atmospheric humidity that caused the TCs precipitation. Moreover, the Cantabrian Sea also supplied large amounts of moisture (~25%).

The probability density function (PDF) of atmospheric particles trajectories that precipitate over the EG-NP region from August to November, calculated by applying the kernel density estimation (KDE) is shown in Fig. 7. As can be seen, the precipitant atmospheric particles over the EG-NP in August (Fig. 7a), frequently traveled from the vicinity

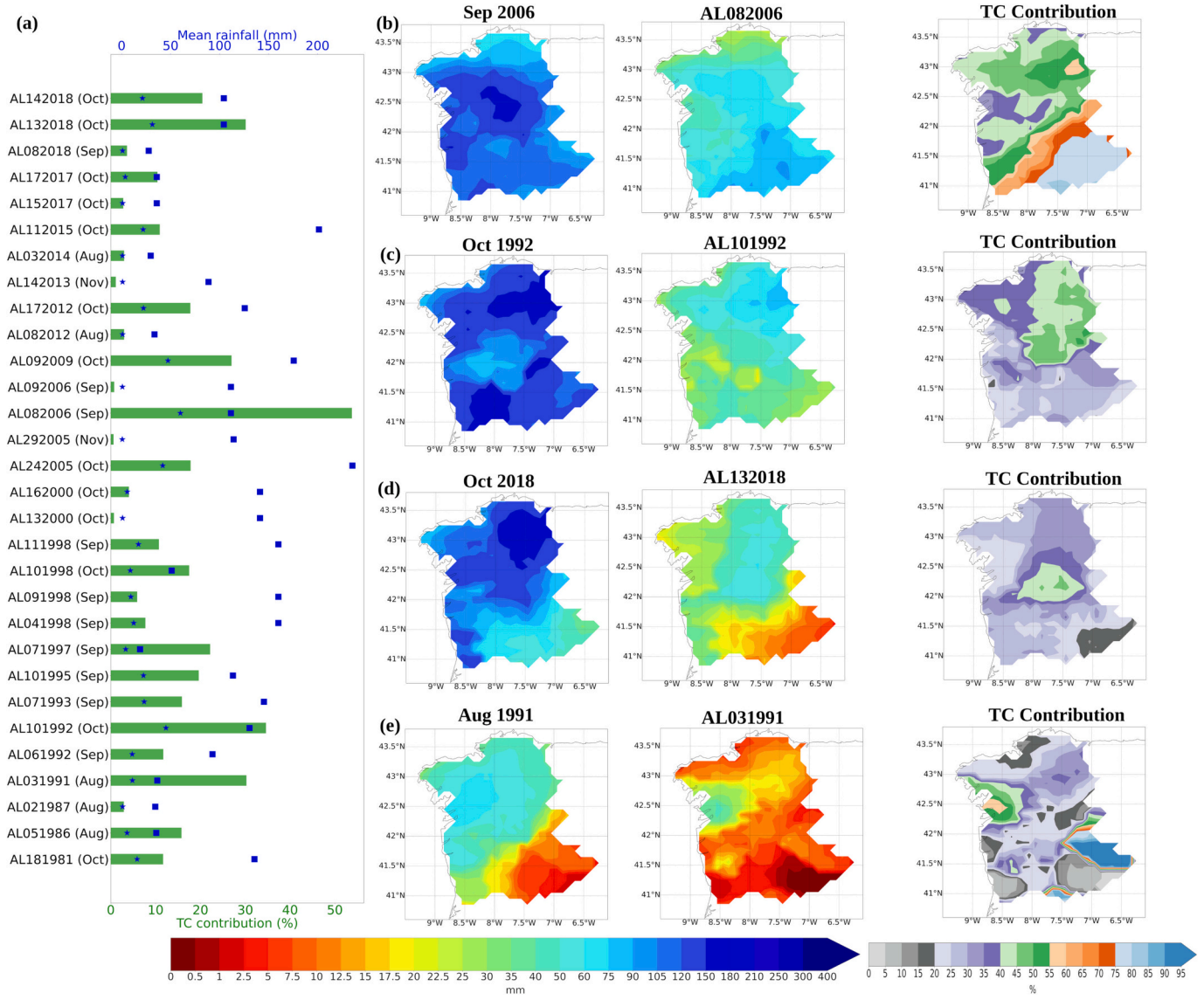

Fig. 5. **(a)** Average monthly rainfall over the Euroregion Galicia - Northern Portugal (blue squares) during the TC passage month, average TC-related precipitation (blue stars) and the percentage of its contribution (green bars) for each TC. In subplots (b-e) are represented the spatial distribution of total rainfall during the TC passage month (left), TC-related precipitation (center) and its contribution in percentage (right) for **(b)** TC Gordon (AL082006), **c)** TC Frances (AL101992), **(d)** TC Leslie (AL132018), and **(e)** TC Bob (AL1991). Rainfall data was obtained from the MSWEP database for the period 1980–2018. (For interpretation of the references to colour in this figure legend, the reader is referred to the web version of this article.)

of the Canary Islands, in the Atlantic Ocean, bordering the Atlantic Morocco coast and over the western IP coast. In September (Fig. 7b), the highest density of trajectories was observed over the IP, in a southeastern-southwestern direction. This pattern suggests that the western Mediterranean Sea is an important moisture source for the precipitation over EG-NP associated with TCs, despite that it has weakly contributed to supplying moisture for the total precipitation over the area within the TC size, as noted above. Furthermore, some precipitating particles arrived at the EG-NP describing a similar trajectory to that observed in August, although with less frequency, and others from the northwestern with origin in the subtropical NATL. During October (Fig. 7c), the highest density of trajectories was found on the Atlantic coast of the IP, while November, again exhibited a totally different pattern to previous months. Due to the small frequency of TC influence on the EG-NP in this last month, note the weak pattern of the trajectory density of precipitant particles from the Cantabrian Sea to the northern EG-NP. Therefore, the analysis for November is of less significance.

Our findings agree with the results from previous studies related to the origin of the precipitation over the whole IP. According to Gimeno et al. (2010), the tropical-subtropical North Atlantic Ocean and the western Mediterranean Sea are the two most important moisture source regions for IP precipitations, however the moisture contribution from these two sources varies throughout the year. The tropical-subtropical North Atlantic Ocean supplied moisture for the IP in winter, but throughout the year for the EG-NP, while the role of the Mediterranean Sea as a moisture source for the precipitation in the study region was restricted to the summer.

4. Summary and conclusions

In this study, we investigated the contribution of tropical-origin cyclones (TCs) to the monthly-accumulated rainfall in the Euroregion Galicia – Northern Portugal (EG-NP), which is located at the northwestern Iberian Peninsula (IP), as well as the origin of TCs-related precipitation during the dates of TC influencing the EG-NP region. To quantify the TC-related rainfall the Multi–Source Weighted–Ensemble

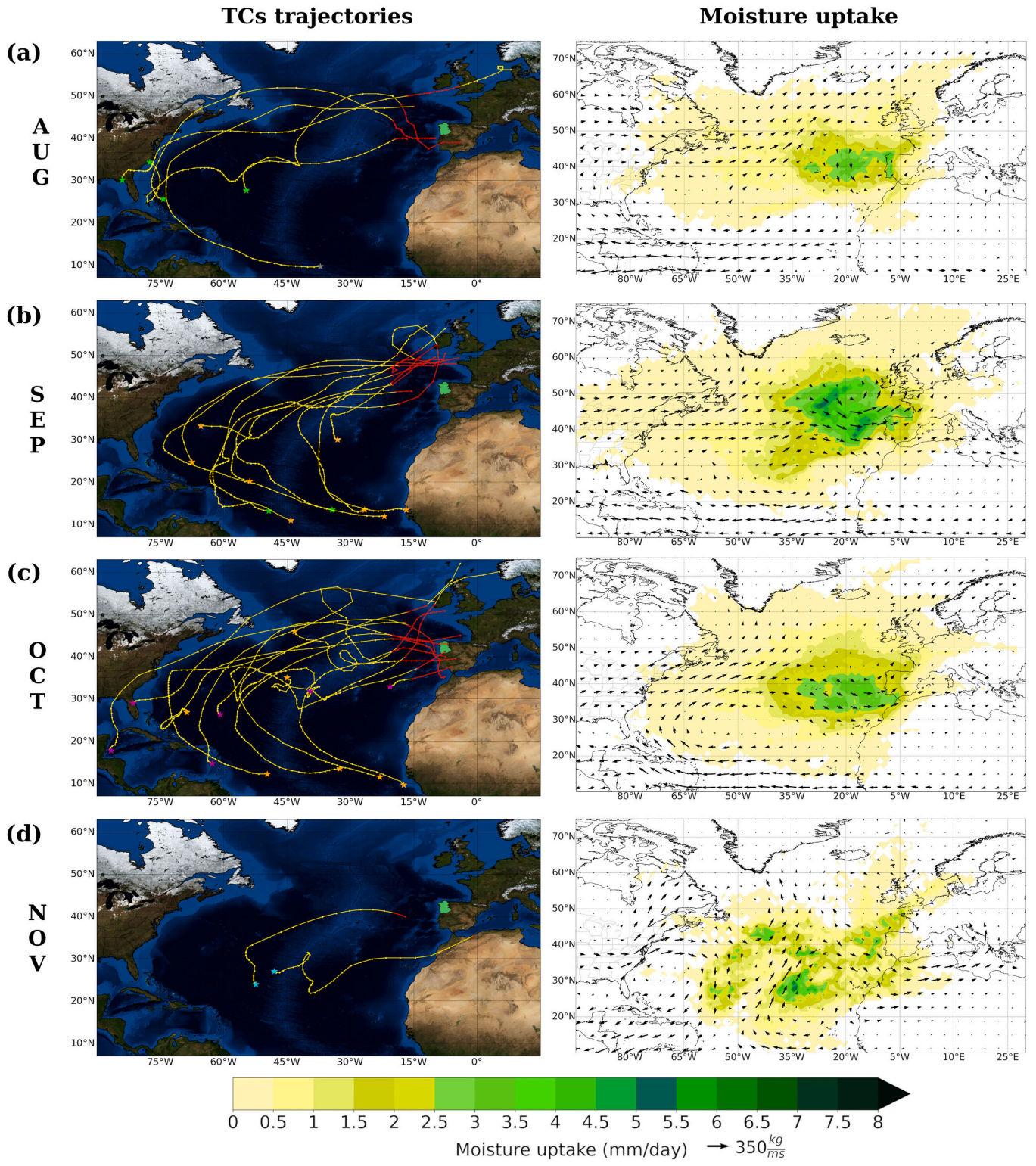

Fig. 6. Trajectories of TCs that influenced the Euroregion Galicia – Northern Portugal (left panel), monthly composites of climatological moisture uptake that originated the tropical-origin cyclones (TCs) related precipitations over the whole area influenced by the TCs size and the VIMF patterns during the TCs passage dates (right panel) for **a)** August, **b)** September, **c)** October and **d)** November.

Precipitation (MSWEP) dataset was used, and to identify the moisture sources for the precipitation associated with TCs the Lagrangian moisture sources diagnostic method implemented in the TRansport Of water Vapor (TROVA) tool was applied. The study period was set from 1980 to 2018 according to the availability of the different databases.

The EG-NP constitutes the westernmost part of Europe, being exposed to the periodic passage of Atlantic storms, i.e., including TCs at the end of their lifetime (Lorenzo et al., 2010b). During the study period, 30 TCs impacted the EG-NP region, which represented ~5% of TCs formed over the North Atlantic basin. Thus, the study region was annually impacted by approximately 0.77 TCs. A simple assessment on the impact of major patterns of ocean-atmosphere circulation was

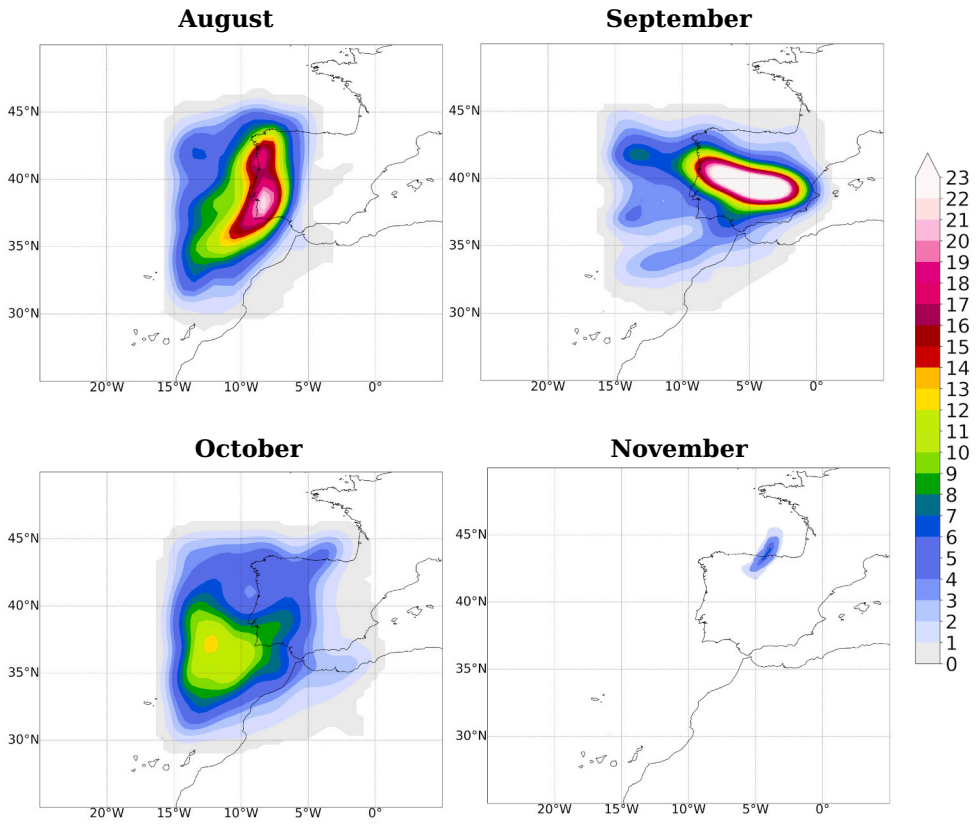

Fig. 7. The probability density function (PDF) (10^{-3}) for the trajectories of atmospheric precipitant particles over the Euroregion Galicia – Northern Portugal during the tropical origin cyclones influence in **(a)** August, **(b)** September, **(c)** October and **(d)** November.

performed. However, we did not find that the climatic variability mode El Niño – Southern Oscillation, neither the North Atlantic Oscillation directly modulated the annual frequency of TC passage. Moreover, the monthly distribution of TC influence ranged from August to November, although September and October exhibited the highest frequency, with 13 and 10 TCs, respectively and November the lowest with 2 TCs. As a general feature, a large fraction of TCs that impacted the EG-NP region often do so after undergoing an extratropical transition. Recently, two important events, Ophelia (Al122017) and Leslie (AL132018), affected western Iberia initially as category 1 hurricane on the Saffir–Simpson wind scale, and later during the extratropical stage.

The contribution of TCs to mean rainfall totals in the EG-NP accounted for ~3.3% in August, ~7.1% in September, ~6.3% in October and less than ~0.5% in November, and an average contribution of 4.2% from August to November. Additionally, the spatial distribution of TCs-related precipitation revealed that the largest contribution occurred in the coastal areas of the western and northern portions of the EG-NP region. On a more individual analysis of important TC events it is worth stressing that Gordon (AL082006) and Frances (AL101992) achieved the largest fractional contribution over the entire study region, accounting for ~51.7% and ~ 34.6% of mean rainfall amounts of September 2006 and October 1992, respectively. Overall, the results show that the western and northern sectors of EG-NP received the largest TCs rainfall contribution.

Finally, the Lagrangian approach used in this study allowed the identification of the origin of the moisture that became TC-related precipitation within the TC outer radius. The precipitant moisture (~75%) mainly came from the subtropical North Atlantic Ocean, especially from the oceanic area close to the coast of IP, driven by the circulation of the North Atlantic Subtropical High pressure system. Likewise, the western Mediterranean Sea and the eastern coast of the United States also contributed, but with less than ~10%. The moisture uptake pattern was almost similar from August to October and slightly different in November, which could be associated with the low frequency of TC passage in this month. Regardless these moisture sources, the atmospheric particles associated with the TCs that precipitated over the EG-NP region traveled from the subtropical North Atlantic Ocean, bordering the Atlantic coasts of Morrocco and IP in August and October. Meanwhile, the western Mediterranean Sea acted as the principal origin of precipitant particles in September, which crossed in southeastern – northwestern direction the IP; and the Cantabrian Sea in November.

It is worth noting that, as TCs do not impact every year the EG-NP region, these findings should be interpreted as an approximation of the role played by TCs on the hydrological cycle in this region and could also support hydrometeorological forecasting for this area. Based on climate projections, these results could be useful for understanding the possible impacts caused by the TCs on the hydrological cycle in the EG-NP under a warmer climate in association with the projected rise of the moisture availability in the atmosphere and precipitation rates of TCs.

Authors statement

Conceptualization: Albenis Pérez-Alarcón, Margarida L. R. Liberato, Luis Gimeno and Raquel Nieto; *Methodology*: Luis Gimeno, Raquel Nieto, Albenis Pérez-Alarcón, Rogert Sorí, Ricardo M. Trigo; *Formal analysis and investigation*: Albenis Pérez-Alarcón, José C. Fernández-Alvarez, Rogert Sorí; *Writing - original draft preparation*: Albenis Pérez-Alarcón; *Writing - review and editing*: Albenis Pérez-Alarcón; Rogert Sorí, Raquel Nieto, Luis Gimeno, José C. Fernández-Alvarez, Margarida L. R. Liberato; Ricardo M. Trigo; *Supervision*: Margarida L. R. Liberato, Luis Gimeno, Raquel Nieto, Ricardo M. Trigo. All authors read and approved the final version of the manuscript.

Funding

This work was supported by the SETESTRELO project under grant no. PID2021-122314OB-I00, funded by the Ministerio de Ciencia, Innovación y Universidades, Spain. Partial support was also obtained from the Xunta de Galicia under the Project ED431C 2021/44 (Programa de Consolidación e Estructuración de Unidades de Investigación Competitivas (Grupos de Referencia Competitiva) and Consellería de Cultura, Educación e Universidade).

Declaration of Competing Interest

The authors declare that they have no known competing financial interests or personal relationships that could have appeared to influence the work reported in this paper.

Data availability

Data will be made available on request.

Acknowledgments

A.P.-A and J.C·F.-A acknowledge the ability to perform this research with the Universidade de Trás-os-Montes e Alto Douro through the European Association for Territorial Cooperation, Galicia Northern Portugal (AECP, GNP) through the IACOBUS program in 2021. A.P-A also acknowledges a PhD grant from the University of Vigo. J.C.F-A acknowledges the support from the Xunta de Galicia (Galician Regional Government) under the grant no. ED481A-2020/193. R.S. acknowledges the support of the postdoctoral fellowship "Ramón y Cajal" no. RYC2021-034044-I, financed by the Ministry of Science and Innovation of Spain. R.M.T was supported by the Portuguese Science Foundation (FCT) through the project ROADMAP (JPIOCEANS/0001/2019). This work has been also possible thanks to the computing resources and technical support provided by CESGA (Centro de Supercomputación de Galicia) and the Red Española de Supercomputación (RES). We acknowledge the funding for open access from the Universidade de Vigo/Consorcio Interuniversitario do Sistema Universitario de Galicia. The authors also thank to anonymous reviewers for their comments and suggestions to improve the manuscript.

References

Algarra, I., Eiras-Barca, J., Miguez-Macho, G., Nieto, R., Gimeno, L., 2019. On the assessment of the moisture transport by the Great Plains low-level jet. Earth Syst. Dynam. 10 (1), 107–119. https://doi.org/10.5194/esd-10-107-2019.

Algarra, I., Nieto, R., Ramos, A.M., Eiras-Barca, J., Trigo, R.M., Gimeno, L., 2020. Significant increase of global anomalous moisture uptake feeding landfalling Atmospheric Rivers. Nat. Commun. 11, 5082. https://doi.org/10.1038/s41467-020-18876-w.

Altman, J., Ukhvatkina, O.N., Omelko, A.M., Macek, M., Plener, T., Pejcha, V., et al., 2018. Poleward migration of the destructive effects of tropical cyclones during the 20th century. Proc. Natl. Acad. Sci. U. S. A. 115 (45), 11543–11548. https://doi.org/10.1073/pnas.1808979115.

Baatsen, M., Haarsma, R., van Delden, A., de Vries, H., 2015. Severe autumn storms in future Western Europe with a warmer Atlantic Ocean. Clim. Dyn. 45, 949–964. https://doi.org/10.1007/s00382-014-2329-8.

Baker, A.J., Hodges, K.I., Schiemann, R.K.H., Vidale, P.L., 2021. Historical variability and lifecycles of North Atlantic midlatitude cyclones originating in the tropics. J. Geophys. Res. Atmos. 126, e2020JD033924 https://doi.org/10.1029/2020JD033924.

Balaguru, K., Foltz, G.R., Leung, L.R., Emanuel, K.A., 2016. Global warming-induced upper-ocean freshening and the intensification of super typhoons. Nat. Commun. 7 (1), 1–8. https://doi.org/10.1038/ncomms13670.

Beck, H.E., Wood, E.F., Pan, M., Fisher, C.K., Miralles, D.G., van Dijk, A.I.J.M., McVicar, T.R., Adler, R.F., 2019. MSWEP V2 global 3–hourly 0.1° precipitation: methodology and quantitative assessment. Bull. Amer. Meteor. Soc. 100, 473–500. https://doi.org/10.1175/BAMS-D-17-0138.1.

Bell, R., Hodges, K., Vidale, P.L., Strachan, J., Roberts, M., et al., 2014. Simulation of the global ENSO–tropical cyclone teleconnection by a high-resolution coupled general circulation model. J. Clim. 27 (17), 6404–6422. https://doi.org/10.1175/JCLI-D-13-00559.1.

Bhardwaj, P., Pattanaik, D.R., Singh, O., 2019. Tropical cyclone activity over Bay of Bengal in relation to El Niño-Southern Oscillation. Int. J. Climatol. 39, 5452–5469. https://doi.org/10.1002/joc.6165.

Bhatia, K.T., Vecchi, G.A., Knutson, T.R., Murakami, H., Kossin, J., Dixon, K.W., Whitlock, C.E., 2019. Recent increases in tropical cyclone intensification rates. Nat. Commun. 2019 (10), 635. https://doi.org/10.1038/s41467-019-08471-z.

Bieli, M., Camargo, S.J., Sobel, A.H., Evans, J.L., Hall, T., 2019. A global climatology of extratropical transition. Part I: Characteristics across basins. J. Clim. 32 (12), 3557–3582. https://doi.org/10.1175/JCLI-D-17-0518.1.

Boudreault, M., Caron, L.P., Camargo, S.J., 2017. Reanalysis of climate influences on Atlantic tropical cyclone activity using cluster analysis. J. Geophys. Res. 122, 4258–4280. https://doi.org/10.1002/2016JD026103.

Colbert, A.J., Soden, B.J., 2012. Climatological variations in North Atlantic tropical cyclone tracks. J. Clim. 25 (2), 657–673. https://doi.org/10.1175/JCLI-D-11-00034.1.

Coll-Hidalgo, P., Pérez-Alarcón, A., Gimeno, L., 2022a. Origin of moisture for the precipitation produced by the exceptional winter storm formed over the Gulf of Mexico in March 1993. Atmosphere 13, 1154. https://doi.org/10.3390/atmos13071154.

Coll-Hidalgo, P., Pérez-Alarcón, A., Nieto, R., 2022b. Moisture sources for the precipitation of tropical-like cyclones in the Mediterranean Sea: a case of study. Atmosphere 13 (8), 1327. https://doi.org/10.3390/atmos13081327.

Ćurić, M., Janc, D., Vujović, D., Vučković, V., 2003. The effects of a river valley on an isolated cumulonimbus cloud development. Atmos. Res. 66 (1–2), 123–139. https://doi.org/10.1016/S0169-8095(02)00144-8.

Daloz, A.S., Camargo, S.J., 2018. Is the poleward migration of tropical cyclone maximum intensity associated with a poleward migration of tropical cyclone genesis? Clim. Dyn. 50, 705–715. https://doi.org/10.1007/s00382-017-3636-7.

Dare, R.A., Davidson, N.E., McBride, J.L., 2012. Tropical cyclone contribution to rainfall over Australia. Mon. Weather Rev. 140, 3606–3619. https://doi.org/10.1175/MWR-D-11-00340.1.

de Castro, M., Lorenzo, N., Taboada, J.J., Sarmiento, M., Alvarez, I., Gomez-Gesteira, M., 2006. Influence of teleconnection patterns on precipitation variability and on river flow regimes in the Miño River basin (NW Iberian Peninsula). Clim. Res. 32 (1), 63–73. https://doi.org/10.3354/cr032063.

Dee, D.P., Uppala, S.M., Simmons, A.J., Berrisford, P., Poli, P., Kobayashi, S., Andrae, U., Balmaseda, M.A., et al., 2011. The ERA-Interim reanalysis: Configuration and performance of the data assimilation system. Q. J. R. Meteorol. Soc. 137, 553–597. https://doi.org/10.1002/qj.828.

Dekker, M.M., Haarsma, R.J., de Vries, H., Baatsen, M., van Delden, A.J., 2018. Characteristics and development of European cyclones with tropical origin in reanalysis data. Clim. Dyn. 50, 445–455. https://doi.org/10.1007/s00382-017-3619-8.

Delgado, S., Landsea, C.W., Willoughby, H., 2018. Reanalysis of the 1954–63 Atlantic Hurricane Seasons. J. Clim. 31, 4177–4192. https://doi.org/10.1175/jcli-d-15-0537.1.

Dominguez, C., Magaña, V., 2018. The role of tropical cyclones in precipitation over the tropical and subtropical North America. Front. Earth Sci. 19 https://doi.org/10.3389/feart.2018.00019.

Eckert-Gallup, A., Martin, N., 2016. Kernel density estimation (KDE) with adaptive bandwidth selection for environmental contours of extreme sea states. In: OCEANS 2016 MTS/IEEE Monterey. IEEE, pp. 1–5. https://doi.org/10.1109/OCEANS.2016.7761150.

Elsner, J.B., Liu, K.B., Kocher, B., 2000. Spatial variations in major US hurricane activity: Statistics and a physical mechanism. J. Clim. 13 (13), 2293–2305. https://doi.org/10.1175/1520-0442(2000)013<2293:SVIMUS>2.0.CO;2.

Emanuel, K., Sobel, A., 2013. Response of tropical sea surface temperature, precipitation, and tropical cyclone-related variables to changes in global and local forcing. J. Adv. Model. Earth Syst. 5, 447–458. https://doi.org/10.1002/jame.20032.

Emanuel, K.A., Živković-Rothman, M., 1999. Development and Evaluation of a Convection Scheme for use in climate Models. J. Atmos. Sci. 56 (11), 1766–1782. https://doi.org/10.1175/1520-0469(1999)056<1766:DAEOAC>2.0.CO;2.

Emanuel, K., Sundararajan, R., Williams, J., 2008. Hurricanes and global warming: results from downscaling IPCC AR4 simulations. B. Am. Meteorol. Soc. 89, 347–367 doi:10.1175.BAMS-89-3-347.

Englehart, P.J., Douglas, A.V., 2001. The role of eastern North Pacific tropical storms in the rainfall climatology of western Mexico. Int. J. Climatol. 21, 1357–1370. https://doi.org/10.1002/joc.637.

Evans, C., Wood, K.M., Aberson, S.D., Archambault, H.M., Milrad, S.M., Bosart, L.F., et al., 2017. The extratropical transition of tropical cyclones. Part I: Cyclone evolution and direct impacts. Mon. Weather Rev. 145, 4317–4344. https://doi.org/10.1175/mwr-d-17-0027.1.

Fernández-Alvarez, J.C., Sorí, R., Pérez-Alarcón, A., Nieto, R., Gimeno, L., 2020. The role of tropical cyclones on the total precipitation in Cuba during the hurricane season from 1980 to 2016. Atmosphere 11, 1156. https://doi.org/10.3390/atmos11111156.

Fernández-Alvarez, J.C., Pérez-Alarcón, A., Nieto, R., Gimeno, L., 2022. TROVA: TRansport of water VApor. SoftwareX 20, 101228. https://doi.org/10.1016/j.softx.2022.101228.

Ferreira-Braz, D., Ambrizzi, T., da Rocha, R.P., Algarra, I., Nieto, R., Gimeno, L., 2021. Assessing the Moisture transports Associated with Nocturnal Low-Level jets in Continental South America. Front. Environ. Sci 9, 657764. https://doi.org/10.3389/fenvs.2021.657764.

Flaounas, E., Fita, L., Lagouvardos, K., Kotroni, V., 2019. Heavy rainfall in Mediterranean cyclones, Part II: Water budget, precipitation efficiency and remote water sources. Clim. Dyn. 53 (5), 2539–2555. https://doi.org/10.1007/s00382-019-04639-x.

Gimeno, L., Nieto, R., Trigo, R.M., Vicente-Serrano, S.M., López-Moreno, J.I., 2010. Where does the Iberian Peninsula moisture come from? An answer based on a Lagrangian approach. J. Hydrometeorol. 11 (2), 421–436. https://doi.org/10.1175/2009JHM1182.1.

Gimeno, L., Stohl, A., Trigo, R.M., Dominguez, F., Yoshimura, K., Yu, L., Drumond, A., Durán-Quesada, A.M., Nieto, R., 2012. Oceanic and terrestrial sources of continental precipitation. Rev. Geophys. 50, RG4003. https://doi.org/10.1029/2012RG000389.

Gimeno, L., Vázquez, M., Eiras-Barca, J., Sorí, R., Stojanovic, M., Algarra, I., et al., 2020. Recent progress on the sources of continental precipitation as revealed by moisture transport analysis. Earth-Sci. Rev. 201, 103070 https://doi.org/10.1016/j.earscirev.2019.103070.

Gimeno, L., Eiras-Barca, J., Durán-Quesada, A.M., Dominguez, F., van der Ent, R.J., Sodemann, H., Sánchez-Murillo, R., Nieto, R., Kirchner, J.K., 2021. The residence time of water vapour in the atmosphere. Nat. Rev. Earth. Environ. 2021 https://doi.org/10.1038/s43017-021-00181-9.

Gómez-Gesteira, M., Gimeno, L., deCastro, M., Lorenzo, M.N., Alvarez, I., Nieto, R., Crespo, A.J.C., Ramos, A.M., Taboada, J.J., Santo, F.E., Barriopedro, D., Trigo, I.F., 2011. The state of climate in NW Iberia. Clim. Res. 48, 109–144. https://doi.org/10.3354/cr00967.

Guo, L., Klingaman, N.P., Vidale, P.L., Turner, A.G., Demory, M., Cobb, A., 2017. Contribution of tropical cyclones to atmospheric moisture transport and Rainfall over East Asia. J. Clim. 30 (10), 3853–3865. https://doi.org/10.1175/JCLI-D-16-0308.1.

Haarsma, R.J., Hazeleger, W., Severijns, C., de Vries, H., Sterl, A., Bintanja, R., van Oldenborgh, G.J., van den Brink, H.W., 2013. More hurricanes to hit western Europe due to global warming. Geophys. Res. Lett. 40, 1783–1788. https://doi.org/10.1002/grl.50360.

Hart, R., Evans, J., 2001. A climatology of the extratropical transition of Atlantic tropical cyclones. J. Clim. 14, 546–564. https://doi.org/10.1175/1520-0442(2001)014<0546:ACOTET>2.0.CO;2.

Hendricks, E.A., Peng, M.S., Fu, B., Li, T., 2010. Quantifying environmental control on tropical cyclone intensity change. Mon. Weather Rev. 138 (8), 3243–3271. https://doi.org/10.1175/2010MWR3185.1.

Hickey, K., 2011. The Impact of Hurricanes on the Weather of Western Europe, Recent Hurricane Research - Climate, Dynamics, and Societal Impacts, Anthony Lupo. IntechOpen. https://doi.org/10.5772/14487.

Jiang, H., Zipser, E.J., 2010. Contribution of tropical cyclones to the global precipitation from eight seasons of TRMM data: Regional, seasonal, and interannual variations. J. Clim. 23, 1526–1543. https://doi.org/10.1175/2009JCLI3303.1.

Jones, P.D., Jónsson, T., Wheeler, D., 1997. Extension to the North Atlantic Oscillation using early instrumental pressure observations from Gibraltar and south-West Iceland. Int. J. Climatol. 17 (13), 1433–1450. https://doi.org/10.1002/(SICI)1097-0088(19971115)17:13<1433::AID-JOC203>3.0.CO;2-P.

Kam, J., Sheffield, J., Yuan, X., Wood, E.F., 2013. The influence of Atlantic tropical cyclones on drought over the eastern United States (1980–2007). J. Clim. 26, 3067–3086. https://doi.org/10.1175/JCLI-D-12-00244.1.

Keller, J.H., Grams, C.M., Riemer, M., Archambault, H.M., Bosart, L., Doyle, J.D., et al., 2019. The extratropical transition of tropical cyclones. Part II: Interaction with the midlatitude flow, downstream impacts, and implications for predictability. Mon. Weather Rev. 147, 1077–1106. https://doi.org/10.1175/mwr-d-17-0329.1.

Khouakhi, A., Villarini, G., Vecchi, G.A., 2017. Contribution of Tropical Cyclones to Rainfall at the Global Scale. J. Clim. 30 (1), 359–372. https://doi.org/10.1175/JCLI-D-16-0298.1.

Kimball, S.K., Mulekar, M.S., 2004. A 15-year climatology of North Atlantic tropical cyclones. Part I: Size parameters. J. Clim. 17, 3555–3575. https://doi.org/10.1175/1520-0442(2004)017<3555:AYCONA>2.0.CO;2.

Klotzbach, P.J., Saunders, M.A., Bell, G.D., Blake, E.S., 2017. North Atlantic seasonal hurricane prediction: Underlying science and an evaluation of statistical models. In: Wang, S., et al. (Eds.), Climate Extremes: Patterns and Mechanisms, Geophysical Monograph Series, 226. American Geophysical Union, Washington DC, pp. 315–328. https://doi.org/10.1002/9781119068020.ch19.

Knutson, T., Camargo, S.J., Chan, J.C.L., Kerry, E., Chang-Hoi, H., James, K., et al., 2019. Tropical cyclones and climate change assessment: Part II. Bull. Am. Meteorol. Soc. 10, 303–332. https://doi.org/10.1175/BAMS-D-18-0194.1.

Kossin, J.P., Olander, T.L., Knapp, K.R., 2013. Trend Analysis with a New Global Record of Tropical Cyclone Intensity. J. Clim. 26, 9960–9976. https://doi.org/10.1175/JCLI-D-13-00262.1.

Läderach, A., Sodemann, H., 2016. A revised picture of the atmospheric moisture residence time. Geophys. Res. Lett. 43, 924–933. https://doi.org/10.1002/2015GL067449.

Landsea, C.W., 2000. El Niño-Southern Oscillation and the seasonal predictability of tropical cyclones. In: Diaz, H.F., Markgraf, V. (Eds.), El Niño and the Southern Oscillation: Multiscale Variability and Global and Regional Impacts. Columbia University Press, New York, pp. 149–181.

Landsea, C.W., Franklin, J.L., 2013. Atlantic hurricane database uncertainty and presentation of a new database format. Mon. Weather Rev. 141, 3576–3592. https://doi.org/10.1175/mwr-d-12-00254.1.

Laurila, T.K., Sinclair, V.A., Gregow, H., 2019. The extratropical transition of Hurricane Debby (1982) and the subsequent development of an intense windstorm over Finland. Mon. Weather Rev. 148, 377–401. https://doi.org/10.1175/mwr-d-19-0035.1.

Liberato, M.L.R., Ramos, A.M., Trigo, R.M., Trigo, I.F., Durán-Quesada, A.M., Nieto, R., Gimeno, L., 2012. Moisture sources and large-scale dynamics associated with a flash flood event. In: Lin, J., Brunner, D., Gerbig, C., Stohl, A., Luhar, A., Webley, P. (Eds.), Lagrangian Modeling of the Atmosphere. https://doi.org/10.1029/2012GM001244.

Liberato, M.L.R., Pinto, J.G., Trigo, R.M., Ludwig, P., Ordóñez, P., Yuen, D., Trigo, I.F., 2013. Explosive development of winter storm Xynthia over the subtropical North Atlantic Ocean. Nat. Hazards Earth Syst. Sci. 13 (9), 2239–2251. https://doi.org/10.5194/nhess-13-2239-2013.

Lima, M.M., Hurduc, A., Ramos, A.M., Trigo, R.M., 2021. The increasing frequency of tropical cyclones in the northeastern atlantic sector. Front. Earth Sci. 9, 745115 https://doi.org/10.3389/feart.2021.745115.

Lorenzo, M.N., Taboada, J.J., 2005. Influences of atmospheric variability on freshwater input in Galician Rias in winter. J. Atmos. Ocean Sci. 10 (4), 377–387. https://doi.org/10.1080/17417530601127472.

Lorenzo, M.N., Taboada, J.J., Iglesias, I., Gómez-Gesteira, M., 2010a. Predictability of the spring rainfall in Northwestern Iberian Peninsula from sea surfaces temperature of ENSO areas. Clim. Chang. 107, 329–341. https://doi.org/10.1007/s10584-010-9991-6.

Lorenzo, M.N., Iglesias, I., Taboada, J.J., Gómez-Gesteira, M., 2010b. Relationship between monthly rainfall in Northwest Iberian Peninsula and North Atlantic Sea surface temperature. Int. J. Climatol. 30 (7), 980–990. https://doi.org/10.1002/joc.1959.

Manganello, J.V., Hodges, K.I., Dirmeyer, B., Kinter, J.L., Cash, B.A., Marx, L., et al., 2014. Future changes in the western North Pacific tropical cyclone activity projected by a multidecadal simulation with a 16-km global atmospheric GCM. J. Clim. 27 (20), 7622–7646. https://doi.org/10.1175/JCLI-D-13-00678.1.

McCloskey, T.A., Bianchette, T.A., Liu, K.B., 2013. Track patterns of landfalling and coastal tropical cyclones in the Atlantic basin, their relationship with the North Atlantic Oscillation (NAO), and the potential effect of global warming. Am. J. Clim. Chang. 2 (3A), 37300. https://doi.org/10.4236/ajcc.2013.23A002.

Montgomery, M.T., Smith, R.K., 2017. Recent developments in the fluid dynamics of tropical cyclones. Annu. Rev. Fluid Mech. 49, 541–574. https://doi.org/10.1146/annurev-fluid-010816-060022.

Murakami, H., Wang, Y., Yoshimura, H., Mizuta, R., Sugi, M., Shindo, E., Adachi, Y., Yukimoto, S., Hosaka, M., Kusunoki, S., Ose, T., Kitoh, A., 2012. Future changes in Tropical Cyclone activity projected by the New High-Resolution MRI-AGCM. J. Clim. 25 (9), 3237–3260. https://doi.org/10.1175/JCLI-D-11-00415.1.

Nieto, R., Gimeno, L., De la Torre, L., Ribera, P., Barriopedro, D., García-Herrera, R., Serrano, A., Gordillo, A., Redaño, A., Lorente, J., 2007. Interannual variability of cut-off low systems over the European sector: the role of blocking and the Northern Hemisphere circulation modes. Meteorog. Atmos. Phys. 96, 85–101 (2007). https://doi.org/10.1007/s00703-006-0222-7.

Numaguti, A., 1999. Origin and recycling processes of precipitating water over the Eurasian continent: experiments using an atmospheric general circulation model. J. Geophys. Res. 104, 1957–1972. https://doi.org/10.1029/1998JD20002.

Papritz, L., Aemisegger, F., Wernli, H., 2021. Sources and transport pathways of precipitating waters in cold-season deep North Atlantic cyclones. J. Atmos. Sci. 78 (10), 3349–3368. https://doi.org/10.1175/JAS-D-21-0105.1.

Pardellas, X.X., Padín, C., 2017. La Eurorregión Galicia-Norte de Portugal y los Modelos de Cooperación Transfronteiriza. Polígonos. Rev. Geogr. 29, 11–35. https://doi.org/10.18002/pol.v0i29.5199.

Parzen, E., 1962. On estimation of a probability density function and mode. Ann. Math. Stat. 33 (3), 1065–1076.

Patricola, C.M., Saravanan, R., Chang, P., 2014. The impact of the El Niño-Southern Oscillation and Atlantic Meridional Mode on seasonal Atlantic tropical cyclone activity. J. Clim. 27, 5311–5328. https://doi.org/10.1175/JCLID1300687.1.

Pérez-Alarcón, A., Sorí, R., Fernández-Alvarez, J.C., Nieto, R., Gimeno, L., 2021. Comparative climatology of outer tropical cyclone size using radial wind profiles. Weather Clim. Extrem. 33, 100366 https://doi.org/10.1016/j.wace.2021.100366.

Pérez-Alarcón, A., Sorí, R., Fernández-Alvarez, J.C., Nieto, R., Gimeno, L., 2022a. Where does the moisture for North Atlantic tropical cyclones come from? J. Hydrometeorol. 23 (3), 457–472. https://doi.org/10.1175/JHM-D-21-0117.1.

Pérez-Alarcón, A., Coll-Hidalgo, P., Fernández-Alvarez, J.C., Sorí, R., Nieto, R., Gimeno, L., 2022b. Moisture sources for precipitation associated with major hurricanes during 2017 in the North Atlantic basin. J. Geophys. Res. Atmos. 127 (4), e2021JD035554.

Pérez-Alarcón, A., Fernández-Alvarez, J.C., Sorí, R., Nieto, R., Gimeno, L., 2022c. Moisture source identification for precipitation associated with tropical cyclone development over the Indian Ocean: a Lagrangian approach. Clim. Dyn. https://doi.org/10.1007/s00382-022-06429-4.

Pérez-Alarcón, A., Sorí, R., Fernández-Alvarez, J.C., Nieto, R., Gimeno, L., 2022d. Moisture source for the precipitation of tropical cyclones over the Pacific Ocean through a lagrangian approach. J. Clim. 36 (4), 1059–1083. https://doi.org/10.1175/JCLI-D-22-0287.1.

Pérez-Alarcón, A., Sorí, R., Fernández-Alvarez, J.C., Nieto, R., Gimeno, L., 2022d. Dataset of outer tropical cyclone size from a radial wind profile. Data Br. 40, 107825 https://doi.org/10.1016/j.dib.2022.107825.

Prat, O.P., Nelson, B.R., 2013. Precipitation Contribution of Tropical Cyclones in the Southeastern United States from 1998 to 2009 using TRMM Satellite Data. J. Clim. 26, 1047–1062.

Ramos, A.M., Lorenzo, M.N., Gimeno, L., 2010. Compatibility between modes of low frequency variability and Circulation Types: a case study of the North West Iberian Peninsula. J. Geophys. Res. 115, D02113. https://doi.org/10.1029/2009JD012194.

Rosenblatt, M., 1956. Estimation of a probability density-function and mode. Ann. Math. Stat. 27, 832–837.

Sainsbury, E.M., Schiemann, R.K., Hodges, K.I., Baker, A.J., Shaffrey, L.C., Bhatia, K.T., 2022. What Governs the Interannual Variability of Recurving North Atlantic Tropical Cyclones? J. Clim. 35 (12), 3627–3641. https://doi.org/10.1175/JCLI-D-21-0712.1.

Schreck, C.J.I.I.I., Knapp, K.R., Kossin, J.P., 2014. The impact of best track discrepancies on global tropical cyclone climatologies using IBTrACS. Mon. Weather Rev. 142, 3881–3899. https://doi.org/10.1175/mwr-d-14-00021.1.

Sharmila, S., Walsh, K.J.E., 2018. Recent poleward shift of tropical cyclone formation linked to Hadley cell expansion. Nat. Clim. Chang. 8, 730–736. https://doi.org/10.1038/s41558-018-0227-5.

Sodemann, H., Schwierz, C., Wernli, H., 2008. Interannual variability of Greenland winter precipitation sources: Lagrangian moisture diagnostic and North Atlantic Oscillation influence. J. Geophys. Res. Atmos. 113, D03107. https://doi.org/10.1029/2007JD008503.

Sorí, R., Vázquez, M., Stojanovic, M., Nieto, R., Liberato, M.L.R., Gimeno, L., 2020. Hydrometeorological droughts in the Miño–Limia–Sil hydrographic demarcation (northwestern Iberian Peninsula): the role of atmospheric drivers. Nat. Hazards Earth Syst. Sci. 20, 1805–1832. https://doi.org/10.5194/nhess-20-1805-2020.

Stewart, S.R., 2018. National Hurricane Center tropical cyclone report. Hurricane. Ophelia AL172017. Retrieved from. https://www.nhc.noaa.gov/data/tcr/AL172017_Ophelia.pdf.

Stohl, A., James, P.A., 2004. Lagrangian analysis of the atmospheric branch of the global water Cycle. Part I: method description, validation, and demonstration for the August 2002 flooding in Central Europe. J. Hydrometeorol. https://doi.org/10.1175/1525-7541(2004)005<0656:ALAOTA>2.0.CO;2, 5,656–678.

Stohl, A., James, P.A., 2005. A Lagrangian analysis of the atmospheric branch of the global water cycle: Part II: Earth's river catchments ocean basins, and moisture transports between them. J. Hydrometeorol. 6, 961–984. https://doi.org/10.1175/JHM470.1.

Stohl, A., Thomson, D.J., 1999. A density correction for Lagrangian particle dispersion models. Bound.-Layer Meteorol. 90 (1), 155–167. https://doi.org/10.1023/A:1001741110696.

Stohl, A., Forster, C., Frank, A., Seibert, P., Wotawa, G., 2005. Technical note: the Lagrangian particle dispersion model FLEXPART version 6.2. Atmos. Chem. Phys. 5, 2461–2474. https://doi.org/10.5194/acp-5-2461-2005.

Studholme, J., Gulev, S., 2018. Concurrent changes to Hadley circulation and the meridional distribution of tropical cyclones. J. Clim. 31, 4367–4389. https://doi.org/10.1175/jcli-d-17-0852.1.

Studholme, J., Hodges, K.I., Brierley, C.M., 2015. Objective determination of the extratropical transition of tropical cyclones in the Northern Hemisphere. Tellus A: Dyn. Meteorol. Oceanogr. 67, 24474. https://doi.org/10.3402/tellusa.v67.24474.

Tan, X., Liu, Y., Wu, X., Liu, B., Chen, X., 2022. Examinations on global changes in the total and spatial extent of tropical cyclone precipitation relating to rapid intensification. Sci. Total Environ. 853, 158555 https://doi.org/10.1016/j.scitotenv.2022.158555.

Trigo, I.F., 2006. Climatology and interannual variability of storm-tracks in the Euro-Atlantic sector: a comparison between ERA-40 and NCEP/NCAR reanalyses. Clim. Dyn. 26, 127–143. https://doi.org/10.1007/s00382-005-0065-9.

Trigo, R.M., Valente, M.A., Trigo, I.F., Miranda, P.M.A., Ramos, A.M., Paredes, D., García-Herrera, R., 2008. The impact of North Atlantic wind and cyclone trends on European precipitation and significant wave height in the Atlantic. Ann. N. Y. Acad. Sci. 1146, 212–234. https://doi.org/10.1196/annals.1446.014.

Valero, F., Martín, M.L., Sotillo, M.G., Morata, A., Luna, M.Y., 2009. Characterization of the autumn Iberian precipitation from long-term datasets: comparison between observed and hindcasted data. International Journal of Climatology: A Journal of the Royal Meteorological Society 29 (4), 527–541. https://doi.org/10.1002/joc.1726.

van Der Ent, R.J., Tuinenburg, O.A., 2017. The residence time of water in the atmosphere revisited. Hydrol. Earth Syst. Sci. 21, 779–790. https://doi.org/10.5194/hess-21-779-2017.

Vecchi, G.A., Knutson, T.R., 2008. On estimates of historical North Atlantic tropical cyclone activity. J. Clim. 21, 3580–3600. https://doi.org/10.1175/2008jcli2178.1.

Vecchi, G.A., Knutson, T.R., 2011. Estimating annual numbers of Atlantic hurricanes missing from the HURDAT database (1878–1965) using ship track density. J. Clim. 24, 1736–1746. https://doi.org/10.1175/2010jcli3810.1.

Vogelezang, D.H.P., Holtslag, A.A.M., 1996. Evaluation and model impacts of alternative boundary-layer height formulations. Bound.-Layer Meteorol. 81 (3), 245–269. https://doi.org/10.1007/BF02430331.

Wahiduzzaman, M., Yeasmin, A., 2020. A kernel density estimation approach of North Indian Ocean tropical cyclone formation and the association with convective available potential energy and equivalent potential temperature. Meteorog. Atmos. Phys. 132, 603–612. https://doi.org/10.1007/s00703-019-00711-7.

Wang, Y.Q., Wu, C.C., 2004. Current understanding of tropical cyclone structure and intensity changes–a review. Meteorol. Atmospheric Phys. 87 (4), 257–278. https://doi.org/10.1007/s00703-003-0055-6.

Węglarczyk, S., 2018. Kernel density estimation and its application. In: ITM Web of Conferences, vol. 23. EDP Sciences. https://doi.org/10.1051/itmconf/20182300037.

Willoughby, H.E., Darling, R.W.R., Rahn, M., 2006. Parametric representation of the primary hurricane vortex. Part II: a new family of sectionally continuous profiles. Mon. Weather Rev. 134, 1102–1120. https://doi.org/10.1175/MWR3106.1.

Winschall, A., Pfahl, S., Sodemann, H., Wernli, H., 2014. Comparison of Eulerian and Lagrangian moisture source diagnostics –the flood event in eastern Europe in May 2010. Atmos. Chem. Phys. 14, 6605–6619. https://doi.org/10.5194/acp-14-6605-2014.

Xu, G., Osborn, T.J., Matthews, A.J., 2017. Moisture transport by Atlantic tropical cyclones onto the North American continent. Clim. Dyn. 48, 3161–3182. https://doi.org/10.1007/s00382-016-3257-6.

Yang, X., Zhou, L., Zhao, C., Yang, J., 2018. Impact of aerosols on tropical cyclone-induced precipitation over the mainland of China. Clim. Chang. 148 (1), 173–185. https://doi.org/10.1007/s10584-018-2175-5.

Zelinsky, D.A., 2019. National Hurricane Center tropical cyclone report. Hurricane Lorenzo (AL132019). Retrieved from. https://www.nhc.noaa.gov/data/tcr/AL132019_Lorenzo.pdf.

Zhang, W., Vecchi, G.A., Murakami, H., Villarini, G., Delworth, T.L., Yang, X., Jia, L., 2018. Dominant role of Atlantic multidecadal oscillation in the recent decadal changes in Western North Pacific tropical cyclone activity. Geophys. Res. Lett. 45, 354–362. https://doi.org/10.1002/2017GL076397.

Zhang, F., Li, G., Yue, J., 2019. The moisture sources and transport processes for a sudden rainstorm associated with double low-level jets in the Northeast Sichuan basin of China. Atmosphere 10 (3), 160. https://doi.org/10.3390/atmos10030160.

Zhang, L., Yang, X., Zhao, J., 2022. Impact of the spring North Atlantic Oscillation on the North Hemisphere tropical cyclones genesis frequency. Front. Earth Sci. 23 https://doi.org/10.3389/feart.2022.829791.

Zhao, M., Held, I.M., 2012. TC-Permitting GCM Simulations of Hurricane Frequency Response to Sea Surface Temperature Anomalies projected for the Late-Twenty-first Century. J. Clim. 25, 2995–3009. https://doi.org/10.1175/JCLI-D-11-00313.1.

Zhao, C., Lin, Y., Wu, F., Wang, Y., Li, Z., Rosenfeld, D., Wang, Y., 2018. Enlarging rainfall area of tropical cyclones by atmospheric aerosols. Geophys. Res. Lett. 45 (16), 8604–8611. https://doi.org/10.1029/2018GL079427.